Stable time-domain boundary integral equation method foraxisymmetric coupled charge-electromagnetic field problems

Stable time-domain boundary integral equation method foraxisymmetric coupled charge-electromagnetic field problems

Stable Time-Domain Boundary Integral Equation Method for Axisymmetric Coupled Charge-Electromagnetic Field Problems

H. Kawaguchi

***Abstract*—In this paper, a stable time-domain boundary integral equation method for transient electromagnetic wave is presented. Careful numerical treatments of the integral equation for stable solution are especially stated. The formulation is given for axisymmetric electromagnetic field problems. A numerical simulation of particle accelerator wake field is also given as an example.**

***Index Terms*—Boundary-element methods, electromagnetic propagation, integral equations, numerical analysis.**

I. Introduction

TIME-DOMAIN numerical simulations of electromagnetic wave phenomena are popularly performed by using the finite-difference time-domain (FDTD) method today. The FDTD method is very powerful simulation scheme, and the required memory size in FDTD is very small. On the other hand, there exist some phenomena which cannot be simulated by FDTD. The coupled problem of electromagnetic wave and charged particles motion is one of such example. In calculating charge current and density from the particle position and velocity, the particle-in-cell (PIC) method often produces numerical noise which causes nonphysical simulation results. For this, the PIC method is not necessary in a boundary integral equation method such as boundary-element method (BEM). To treat these kinds of problems, the author has been working on a time-domain boundary integral equation (TDBIE) method, and presented a formulation of TDBIE and numerical simulation examples as well [1], [2]. However, the method still has a problem of numerical instabilities in the long time range. Indeed, there exist no stable scheme of time-domain BEM except for special cases (e.g., electromagnetic wave scattering problem from thin wires [3]). In this paper, a stable TDBIE for long-time range is presented. Owing to implicit property of the stable scheme, its required memory size becomes quite larger and three-dimensional (3-D) simulation is impossible even in a supercomputer. A formulation of axisymmetric systems is presented here.

Manuscript received July 5, 2001; revised October 25, 2001. This work was supported in part by Japan Society for the Promotion of Science under Grant-in-Aid 13640251 for Scientific Research.

The author is with the Department of Electrical and Electronic Engineering, Muroran Institute of Technology, Muroran 050-8585, Japan (e-mail: kawa@mmm.muroran-it.ac.jp).

Publisher Item Identifier S 0018-9464(02)01236-0.

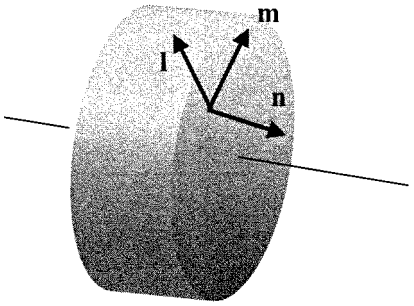

Fig. 1. Local coordinate on boundary surface.

II. Boundary Integral Equations

There are three unknowns on the (perfect conductor) boundary surface, i.e., surface charge density $\boldsymbol{\sigma}$ and two components of surface current density $\boldsymbol{K}$. Two of these values are independent because of the continuity equation

$$\frac{\partial \sigma}{\partial t} + \mathrm{div}\boldsymbol{K} = 0. \tag{1}$$

Then the electromagnetic field is described by the following time-domain boundary integral equation (which is a kind of Kirchhoff's equation) [1], [2]:

$$\boldsymbol{B}(t.\boldsymbol{x}) = \boldsymbol{B}_{\mathrm{ext.}}(t, \boldsymbol{x}) - \frac{1}{4\pi}\int_S dS' \left[\frac{(\boldsymbol{x}-\boldsymbol{x}')}{|\boldsymbol{x}-\boldsymbol{x}'|^3} + \frac{(\boldsymbol{x}-\boldsymbol{x}')}{|\boldsymbol{x}-\boldsymbol{x}'|^2}\frac{\partial}{c\partial t}\right] \times \boldsymbol{B}_t\left(t - \frac{|\boldsymbol{x}-\boldsymbol{x}'|}{c}, \boldsymbol{x}'\right) \tag{2}$$

where $\boldsymbol{B}_{\mathrm{ext}}$ is external magnetic field which is produced by electric current or incoming wave. The value $\boldsymbol{B}_t$ is the tangential components of the magnetic field on the boundary surface, which are directly related to the surface current $\boldsymbol{K}$ by

$$\boldsymbol{K} = \varepsilon_0 c^2(\boldsymbol{B} \times \boldsymbol{n}) \tag{3}$$

(where $\boldsymbol{n}$ is unit normal vector on the boundary). Here, we shall assume that the numerical model has axisymmetric structure. To explicitly express (2) by using independent components of $\boldsymbol{B}_t$, we shall introduce a local coordinate shown in Fig. 1. The unit vector $\boldsymbol{m}$ is oriented to the θ-direction and lies on the boundary surface. The vector $\boldsymbol{l}$ also lies on the boundary and is perpendicular to both $\boldsymbol{n}$ and $\boldsymbol{m}$. Then, $\boldsymbol{K}$ and $\boldsymbol{B}_t$ are expressed by using two components as follows:

$$\boldsymbol{B}_t = B_m\boldsymbol{m} + B_l\boldsymbol{l} \tag{4}$$

$$\boldsymbol{K} = K_m\boldsymbol{m} + K_l\boldsymbol{l}. \tag{5}$$

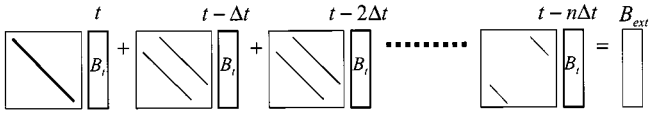

Fig. 2. System matrix configuration.

The integral equation (2) is then explicitly expressed by two tangential components of magnetic field as follows:

$$\boldsymbol{B}(t,\boldsymbol{x}) = \boldsymbol{B}_{\text{ext.}}(t,\boldsymbol{x}) - \frac{1}{4\pi}\int_S dS' \cdot \left\{ [(\boldsymbol{R}\cdot\boldsymbol{n})\boldsymbol{m} - (\boldsymbol{R}\cdot\boldsymbol{m})\boldsymbol{n}] B_m\left(t - \frac{|\boldsymbol{x}-\boldsymbol{x}'|}{c}, \boldsymbol{x}'\right) + [(\boldsymbol{R}\cdot\boldsymbol{n})\boldsymbol{l} - (\boldsymbol{R}\cdot\boldsymbol{l})\boldsymbol{n}] B_l\left(t - \frac{|\boldsymbol{x}-\boldsymbol{x}'|}{c}, \boldsymbol{x}'\right)\right\} \quad (6)$$

where

$$\boldsymbol{R}(\boldsymbol{x},\boldsymbol{x}') = \frac{(\boldsymbol{x}-\boldsymbol{x}')}{|\boldsymbol{x}-\boldsymbol{x}'|^3} + \frac{(\boldsymbol{x}-\boldsymbol{x}')}{|\boldsymbol{x}-\boldsymbol{x}'|^2}\frac{\partial}{c\partial t}. \quad (7)$$

For axisymmetric systems, (6) is simplified as follows [4]:

$$\boldsymbol{B}(t.\boldsymbol{x}) = \boldsymbol{B}_{\text{ext.}}(t,\boldsymbol{x}) - \frac{1}{4\pi}\int_S dS'(\boldsymbol{n}\cdot\boldsymbol{R}) B_m\left(t - \frac{|\boldsymbol{x}-\boldsymbol{x}'|}{c}, \boldsymbol{x}'\right)\boldsymbol{m}. \quad (8)$$

Owing to the retarded property of (6) and (8), the boundary values $\boldsymbol{B}_t$ at different time are independent of each other. Therefore, discretization of (6) or (8) for both of time and spatial axes yields the matrix equation as in Fig. 2. The value $\boldsymbol{B}_t$ at time t is then calculated by using the previous values at time $t-\Delta t, t-2\Delta t, \ldots, t-n\Delta t$.

III. Formulation of Numerical Simulation

In real numerical simulation, the observation point $\boldsymbol{x}$ in (6) or (8) is moved to each boundary element $\boldsymbol{x}'$ and the matrix equation is constructed according to standard BEM scheme. However, some practical considerations are required to obtain stable solutions for long-time range. In FDTD, a simulation is performed on a grid structure. Then Maxwell's equation are well expressed in the discretized grid space [5]. On the other hand, strict expression of Maxwell's equation is impossible on general unstructural meshes as in BEM or FEM. This difficulty appears as a numerical instability for long-time range in the time-domain BEM or FEM. Especially strict numerical evaluations of the conservation law (continuity equation) and causality relation are needed for stable solution in time-domain BEM.

A. Allocation of Unknown Variables

An allocation of the surface charge and current components is shown in Fig. 3(a). The values of current components are assumed to be constant on the edge and the charge density is also constant on the mesh. This allocation will lead us to natural evaluation of the continuity equation. This is the same idea as the finite-volume approximation in the Computational Fluid Dynamics (CFD). The allocation of the associated magnetic field components on the boundary surface is shown in Fig. 3(b). According to this allocation of the magnetic field components,

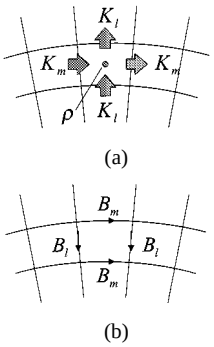

Fig. 3. (a) Allocation of surface charge and current density. (b) Allocation of associated magnetic field components.

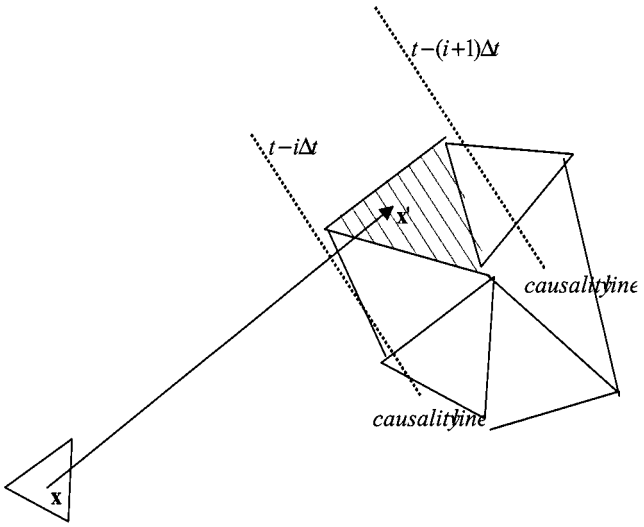

Fig. 4. Boundary element and causality lines.

the calculation of value of $|\boldsymbol{x}-\boldsymbol{x}'|$ should be properly evaluated in (6) or (8).

B. Causality Relation

The following condition should be satisfied for short-time range stability [1]

$$c\Delta t \geq \Delta l \quad (9)$$

where Δt is the unit time step and Δl is the maximum mesh size (the inequality is opposite direction to that of the standard FDTD stable condition). In addition to the condition (9), $c\Delta t$ should be almost the same size as Δl. Therefore, there exists a time difference in the value of $|\boldsymbol{x}-\boldsymbol{x}'|/c$ between one corner and another corner of a mesh (see Fig. 4). In that case, the Gauss–Legendre-type numerical integral cannot be applied for (6) or (8). Then subdiscretization of the mesh should be done along to the causality lines in the numerical integration (see Fig. 4).

C. Implicit Scheme

In addition to careful evaluation of the conservation law and causality relation, an implicit scheme in time evolution calculation is necessary for stable simulation. This implicit scheme is expressed in the form of a big matrix equation of Fig. 5. Each line of the matrix is just corresponding to the matrix equation

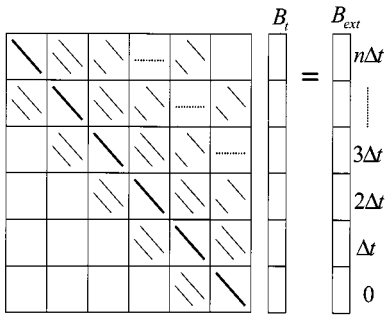

Fig. 5. Matrix expression of implicit scheme.

of Fig. 2. Then many iteration calculations should be performed until converged solutions are obtained. Accordingly, the calculation is of a very large size, and CPU time is very big even in axisymmetric simulations.

IV. Reduction of the 3-D Problem to a 2.5-D Problem

A full 3-D simulation of (6) is almost impossible even in any present-day supercomputers from the viewpoint of CPU time and memory capacity. If the number of nodes for one dimension size of an object is n, the number of boundary elements of the numerical model is of the order n^2. Then, the required memory is $n^4 \times m$, when the number of matrices in Fig. 2 is m. For example, the required memory is 40 GB for $n = 100$ and $m = 100$. This amount is much bigger than memory capacity of any present-day supercomputers. On the other hand, the number of nodes is of order $n^2 \times m$, when the system is axisymmetric (2-D). In this case, the memory requirement is 4 MB, which is small enogh even for PCs. Furthermore, a big memory reduction can be done even in 3-D field calculation if the object has an axisymmetric structure. When the numerical model is axisymmetric, the relation between A and A' or A'' in Fig. 6(a) is the same as that of B and B' or B''. Then the matrix is partially symmetric. Line 2 in the matrix of Fig. 6(b) is just a rotational right shift of line 1 by one element, and we do not need to store line 2 in the memory. This is so-called 2.5-dimensional (2.5-D) simulation. In this case, the required memory is $n^3 \times m$, and it becomes 500 MB for $n = 100$ and $m = 100$. This is small enough for the memory capacity of easily available high-performance computers.

V. Numerical Examples

In this section, a numerical example based on the formulation in the previous section is shown. A typical example of coupled problems of a charged particle and an electromagnetic wave is the wake field in particle accelerators. Fig. 7(a) shows the cross section of a particle accelerator disk load structure. It is assumed that the charged particle has Gaussian bunch shape of 3-mm size, and is running with 99.994% of light velocity. Then, the electromagnetic fields produced by charged particles are trapped by the cavity structure after the particle has passed though the cavity. When the charged particle motion lies on the center axis, the electromagnetic field is axisymmetric and (8) can be used for simulation. Fig. 7(b) shows a 3-D numerical model of the dotted line part in Fig. 7(a). In this case, one dimension size n is about 200 and the required memory size is

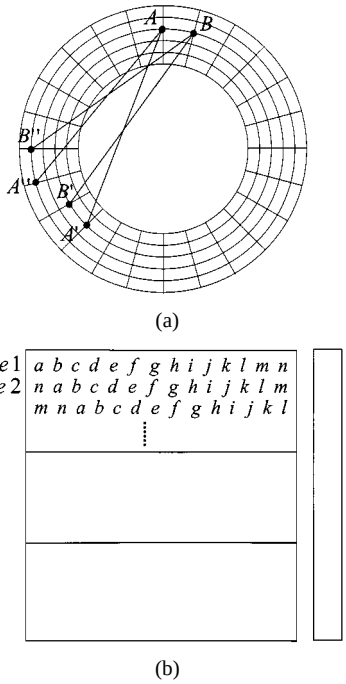

Fig. 6. (a) Rotational symmetry in an axisymmetric structure. (b) Symmetry in matrix of an axisymmetric object.

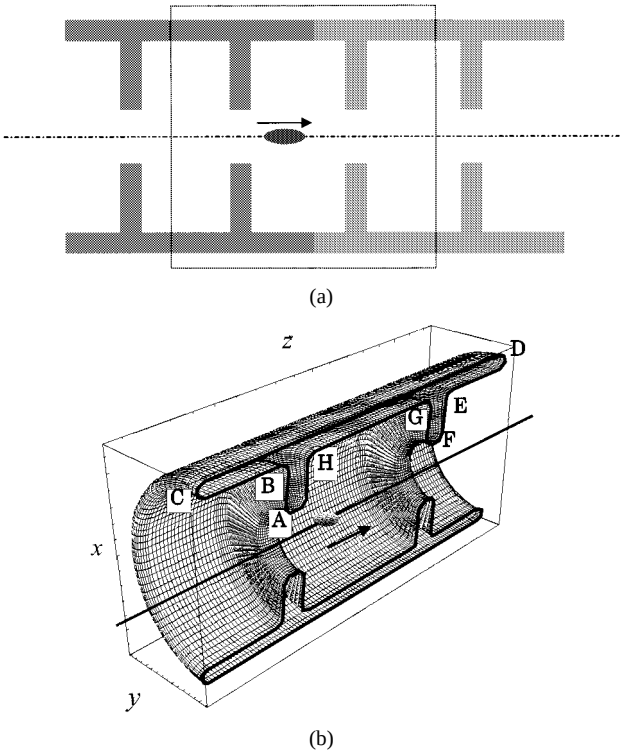

Fig. 7. (a) Cross section of an axisymmetric accelerator cavity. (b) 3-D numerical model of an accelerator cavity.

about 2 GB. The most important value in this simulation is the time evolution of surface current and density. Fig. 8 shows the time evolution of current density distribution on the cross section boundary [A-B-C-D-E-F-G-H-A in Fig. 7(b)]. The notations A to H on the axis in Fig. 8 are corresponding to specified positions on the cross section in Fig. 7(b). A-H-G-F is then a

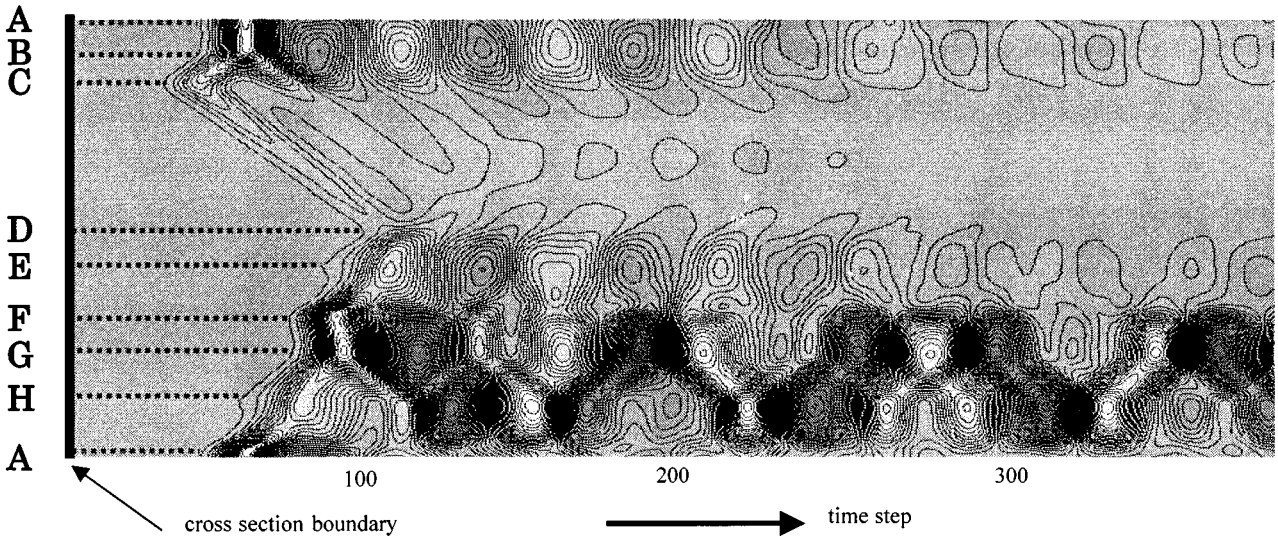

Fig. 8. Time evolution of surface current density.

cavity part. It is well simulated that the electromagnetic field is trapped by the cavity for a long time in Fig. 8.

VI. Summary

This paper has presented a stable TDBIE for 2- and 2.5-D electromagnetic fields. Numerical example of 2-D simulation has been also presented for a particle accelerator wake field. The numerical simulation for 2.5 dimensions is possible from the viewpoint of memory capacity, but it takes a very long computation time (about several days by a supercomputer). The 2.5-D simulation by a parallel computing machine is now under consideration, and will be presented in the near future.

References

[1] H. Kawaguchi and T. Honma, "Consideration on numerical instability of Dirichlet gauge BEM," *IEEE Trans. Magn.*, vol. 32, pp. 914–917, 1996.

[2] H. Kawaguchi, M. Isoda, and T. Honma, "Implicit scheme time domain BEM analysis of transient electromagnetic fields," in *Boundary Element XIX*, M. Marchett, C. A. Brebbia, and M. H. Aliabadi, Eds., 1997, pp. 477–484.

[3] E. K. Miller, A. J. Poggio, and G. J. Burke, "An integro-differential equation technique for the time-domain analysis of thin wire structures, I. The numerical method," *J. Comp. Phys.*, vol. 12, pp. 44–48, 1973.

[4] A. V. Novokhatski, "On the estimation of the wake potential for an ultrarelativistic charge in an accelerating structure," in *Institute of Nuclear Physics*: Novosibirsk Preprint, 1988, vol. 88.

[5] T. Weiland, "Time domain electromagnetic field computation with finite difference methods," *Int. J. Numer. Modeling: Electronic Networks: Electronic Network, Devices and Fields*, vol. 9, pp. 295–319, 1996.